Controlling Photon Echo in a Quantum-Dot Semiconductor Optical Amplifier Using Shaped Excitation

A. K. Mishra,[1] O. Karni,[2] I. Khanonkin,[1] and G. Eisenstein[1]

[1]*Andrew and Erna Viterby Department of Electrical Engineering and Russell Berrie Nanotechnology Institute, Technion-Israel Institute of Technology, Haifa 32000, Israel*

[2]*E. L. Ginzton Laboratory, Applied Physics Department, Stanford University, Stanford, California 94305, USA*

(Received 31 January 2017; revised manuscript received 26 March 2017; published 12 May 2017)

Two-pulse photon-echo-based quantum-memory applications require a precise control over the echo strength and appearance time. We describe a numerical investigation of observation and control of photon echo in a room-temperature InAs/InP–based quantum-dot (QD) semiconductor optical amplifier (SOA). We address an important case where the spectral excitation is narrower than the inhomogeneous broadening of the SOA. It is revealed that, in such a QD SOA, the amplitude of the echo pulse depends not only on the excitation-to-rephasing pulse temporal separation but also on the interference among the rephrasing pulse and the echo pulses generated during the propagation along the amplifier. More importantly, the appearance time and amplitude of the echo pulse can be precisely controlled by shaping the first (excitation) pulse. We also assert that deviations in the echo pulse stemming from the SOA gain inhomogeneity can be compensated for so as to be utilized in quantum coherent information processing.

DOI: 10.1103/PhysRevApplied.7.054008

I. INTRODUCTION

Photon echo, the optical analogue of spin echo, is a quantum-mechanical manifestation of a reversible nonlinear light-matter interaction, which is a form of a quantum memory [1–5]. The phenomenon has long been studied in semiconductors for the purpose of quantum-memory applications, as well as for the extraction of different carrier relaxation processes [6]. The prerequisite for the manifestation of photon echo is a broad distribution of transitions. An inhomogeneously broadened ensemble of states in quantum-dot (QD)-based devices meet this criteria; they also provide a practical platform to perform photon-echo-based experiments and study their potential applications [7–9].

In an idealized atomic system, an excitation pulse of $\pi/2$ area sets up a coherent electronic state which dephases with time due to the ensemble inhomogeneity. A subsequent π-area pulse, delayed in time by τ_{12}, inverts the evolution of the dipoles leading to the formation of an echo pulse exactly τ_{12} after the second pulse, as shown schematically in Fig. 1. When the finite width (t_0) of pulses is also considered, the echo signal is delayed by $t_0 + \tau_{12}$.

Contrary to several other quantum-memory-storage protocols, photon echo does not require any initial-state preparation, and it rephases any random distribution of states without any assumption about the source of inhomogeneity. Furthermore, because of the selective excitation determined by the spectral content of the first pulse, a spectral selection within the inhomogeneously broadened spectrum is inherent in photon echo [5].

Photon echo has been observed experimentally in various systems at cryogenic and room temperatures [6,8–11]. The case of resonant excitation of an inhomogeneous ensemble of QDs is well studied and understood. Time-resolved four-wave-mixing studies in an electrically pumped room-temperature InAs/(In, Ga)As/GaAs QD semiconductor optical amplifier (SOA) yielded a delayed photon-echo signature resulting from the dominant inhomogeneous broadening at low bias [11]. Recently, it was observed that in a highly inhomogeneous (In, Ga)As/GaAs QD ensemble, where the pulse spectrum is such that it addresses almost all of the QDs resonantly, the formation of the echo strongly depends on the area of the exciting pulse [12].

Storage and manipulation of quantum information requires precisely timed pulse sequences, and a determination of the echo-signal appearance time with utmost accuracy is therefore of vital importance [12]. Any control over the timing for a system where the excitation spectrum is narrower than the spectral extent of transitions, defying a dependence of the echo appearance time on the excitation pulse area, emanates either from τ_{12} variation or from

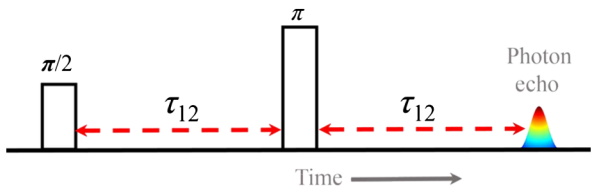

FIG. 1. Schematic representation of conventional two pulse photon echo. The excitation (first) pulse area is $\pi/2$ and the rephrasing (second) pulse area is π. τ_{12} represents the temporal separation between the two pulses.

changes in the carrier-density-driven medium parameters. Therefore, it is important to study the effects of shaping the excitation pulse on the echo formation in any distributed system—particularly in practical room temperature InAs/InP–based QD SOAs, which are considered here.

Advances in growth technology avail InAs/InP QDs of reduced size fluctuation, which in turn leads to an optical-gain material with a reduced inhomogeneous linewidth [13]. A SOA is a distributed device, and its use for studies of coherent dynamics is therefore complicated because of the need to consider the propagation effects. We have previously studied the combination of Rabi oscillation and self-induced transparency which takes place in the presence of incoherent effects, e.g., group velocity dispersion (GVD) and two-photon absorption (TPA), with its associated Kerr effect. These phenomena are analyzed on an ultrashort time scale for a short pulse propagating along a room-temperature InAs/InP–based QD SOA [14,15]. Recently observed coherent signatures [15] and their manipulation through shaped pulses [16,17] have made these practical optoelectronic devices a viable platform for performing different quantum-coherent experiments.

In this work, we numerically explore the possibility of controlling two-pulse photon echoes in an InAs/InP–based QD SOA with moderate inhomogeneous broadening using pulses of relatively narrow spectral width. These pulses eliminate any possibility of variation in the echo signal timing with the change in the input area of the excitation pulse [12]. Propagation-induced phase accumulation leads to a periodic dependence of the echo-pulse intensity on the temporal separation between the excitation and rephrasing pulses (τ_{12}). For a fixed τ_{12}, a varying quadratic spectral phase (QP) of the excitation pulse is used to analyze changes in the echo pulse for three spectral locations of the pulse center: at the minimum of the SOA's absorption spectrum, on the short-wavelength side of the absorption minimum and on the long-wavelength side of the same. We observed that this kind of shaping of the excitation results in a variation of both the echo intensity and its appearance time.

II. NUMERICAL MODEL

The light-matter interaction along the length of an electrically driven QD SOA is analyzed using a previously developed numerical model which treats the interactions within a semiclassical framework [16]. The model employs a finite-difference time-domain algorithm and calculates the evolution of the electromagnetic field and the ensemble of electronic states of inhomogeneously broadened effective two-level systems by solving the Maxwell and Schrödinger equations in the density-matrix formalism without resorting to either the slowly evolving or the rotating-wave approximation. Inhomogeneity is incorporated by defining a set of conduction band edges whose distribution is determined from experiments. For each two-level system, the model assumes one excited state associated with the ground state of the electrons in the QDs. The QDs are coupled to a common carrier reservoir through different carrier capture and the escape processes whose rates are governed by the detailed-balance principle [18]. Although the QDs are not coupled directly to each other, an indirect coupling, mediated by the carrier reservoirs, exists. The incoherent carrier dynamics among QD ground states, excited states, electrically fed carrier reservoirs and TPA injection levels are treated by a set of rate equations.

The nonresonant effects (GVD and TPA and its associated Kerr effect) contribute through the polarization term in the Maxwell equations and are described by coupled differential equations. The electromagnetic wave interacts with the active medium through the potential term of the Schrödinger equation, while the medium imprints its response on the wave through the polarization term of Maxwell's equation. The details of the model can be found in previous publications [14–16].

III. RESULTS AND DISCUSSION

Transform-limited (TL) Gaussian pulses with a FWHM of 150 fs are used as excitation and rephasing pulses. The homogeneous and inhomogeneous linewidths of the QD ensemble are taken as 7 and 30 nm, respectively. The Gaussian absorption profile of the QD SOA is centered at 1580 nm. All of the photon-echo studies are performed in the absorption regime with a fixed SOA bias of 10 mA. The pulses are spectrally located at the absorption minimum of the QD SOA, i.e., at 1580 nm as well as at 1540 and 1600 nm. The simulation parameters are the same as those given in Ref. [16].

Since the SOA is a distributed system, the echo signal forms as soon as the second pulse enters the device, and, with further propagation, the echo is modified due to an interaction with newly generated echo signals and with the rephasing pulse. The dependence of the echo signal on the separation between the excitation and the rephrasing TL pulse is shown in Fig. 2(a). The upper part of Fig. 2(a) shows intensity profiles, while the lower part exhibits the corresponding instantaneous frequency (chirp). Each input separation is varied by 3 fs (which is roughly half of the single-cycle duration at 1580 nm) in order for the interference to consequently revert its phase.

The vertical scale in Fig. 2(a) submerging the echo is very large, so an enlarged image is presented as Fig. 2(b), where the echo signals are shown to be 2 orders of magnitude smaller in intensity than those of the original pulses. Furthermore, as the separation between the first two pulses is varied by 3 fs, both the strength and the appearance time of the echo signals change drastically [for example, compare the solid blue (300-fs) and dashed blue (303-fs) curves] clearly indicating that its origin is in interference. This abrupt change in the echo signal emphasizes the importance of choosing a correct separation

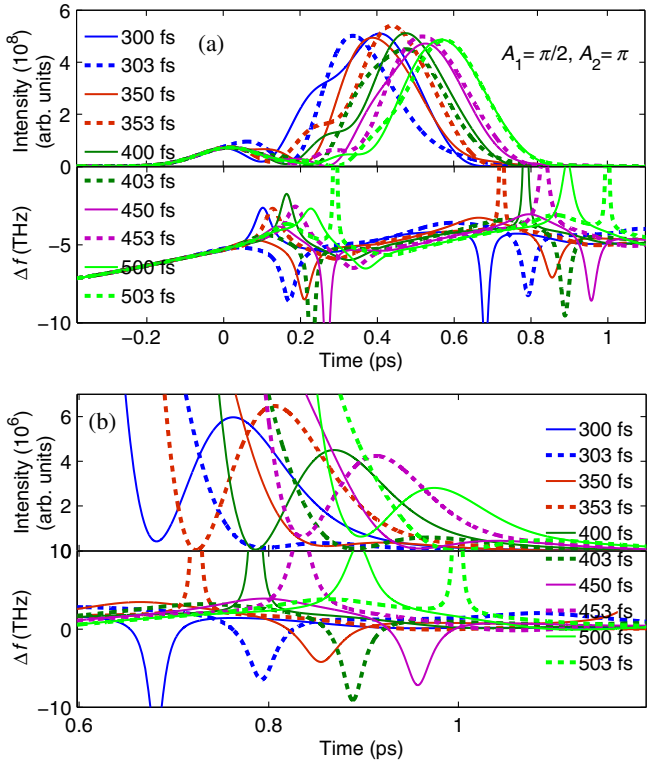

FIG. 2. (a) Simulated output intensity and instantaneous-frequency profiles of excitation ($\pi/2$ area) and rephrasing (π area) pulses centered at 1580 nm with varying input separation. (b) Enlarged view of (a) after the rephrasing pulse.

between the excitation and rephrasing pulses in order to observe a strong photon echo in a distributed device.

The case we are analyzing considers an inhomogeneous spectral width, δ, which is wider than the spectral extent of the excitation pulse of temporal width t_0, so $t_0\delta \approx 0.5$. A value of $t_0\delta$ which is less than one guarantees no variation in the appearance time of the echo with the change in the area of the first (excitation) pulse [12]. This claim is verified in Fig. 3, where, for the fixed separation between the two pulses (453 fs), the area of the first pulse is varied and the appearance time of the echo is identified. The echoes appear at almost the same time (under the constraint set by the interference), irrespective of the area of the first pulse. This independence on area ascertains that whatever study is performed here onwards, any change in the appearance time of the echo signal does not originate from the variations in the excitation pulse area [12].

Control over both the strength and the appearance time of the echo for a fixed separation between the first two pulses is investigated by shaping the first pulse while keeping the second pulse TL. QPs of different magnitudes and signs are imposed to realize the shaping numerically. A negative QP introduces positive chirp and a positive QP a negative chirp in the temporal profile of the pulse; obviously, the introduction of chirp broadens the input pulse. Moreover, the rephasing pulse always broadens

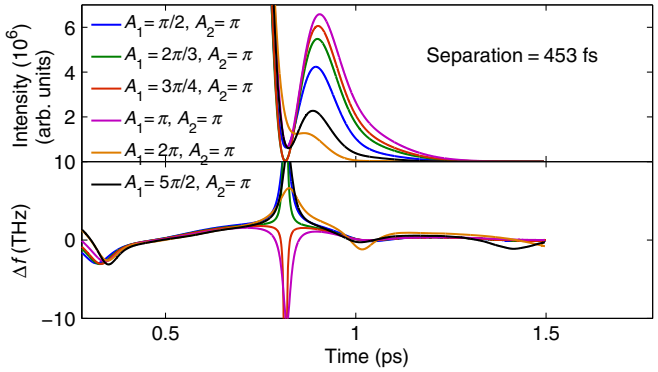

FIG. 3. Simulated output intensity and instantaneous-frequency profiles of an echo signal appearing after excitation and rephrasing (π-area) pulses centered at 1580 nm with varying excitation pulse areas. The temporal separation between the excitation and rephrasing pulses is 453 fs.

while propagating along the SOA; imposing a QP would stretch it further so that its trailing edge would submerge the echo. Hence, in this study, only the first pulse is shaped. A properly formed, maximum-amplitude echo determines the optimum separation between the two TL input pulses; keeping this separation fixed while shaping the excitation pulse allows us to observe the evolution of the echo.

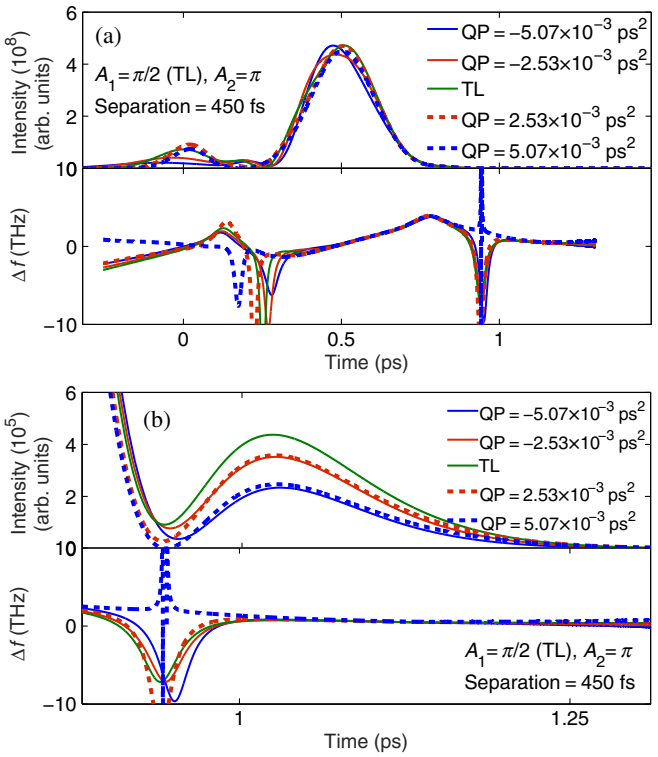

FIG. 4. (a) Simulated output intensity and instantaneous-frequency profiles of excitation and rephrasing (π-area) pulses centered at 1580 nm with varying input QPs of the excitation pulse. The temporal separation between the excitation and the rephrasing pulses is 450 fs. (b) Enlarged view of (a) after the rephrasing pulse.

Figure 4(a) shows the output intensity and the instantaneous-frequency profiles of pulses separated by 450 fs at the input of the amplifier and centered at 1580 nm, with the first pulse being shaped. A_1 and A_2 represent, respectively, the areas of the first and second input pulses in their TL form. The area of the first pulse in its TL form is $\pi/2$. QPs of different magnitudes and signs are introduced in the first pulse, as depicted in Fig. 4(a). An enlarged image of Fig. 4(a) after the second pulse is shown in Fig. 4(b), which reveals that the strength of the echo signal strongly depends on the magnitude of the QP of the first pulse, but the appearance time does not. Such a dependence of the echo signal on excitation pulse QP implies that, for pulses centered at the SOA absorption minimum, the amplifier, because of spectral symmetry, does not differentiate the spectral sequence of interaction. Moreover, a larger QP at the input leads to broader pulses, which, in turn, leads to a weaker interaction with the SOA medium, and this further results in a weaker echo.

Figures 5(a) and 5(b) depict a similar study, but for pulses with a different input separation (550 fs). For larger separations, the echo is weaker [compared to that in Fig. 4(b)], consistent with more dephasing of the coherence.

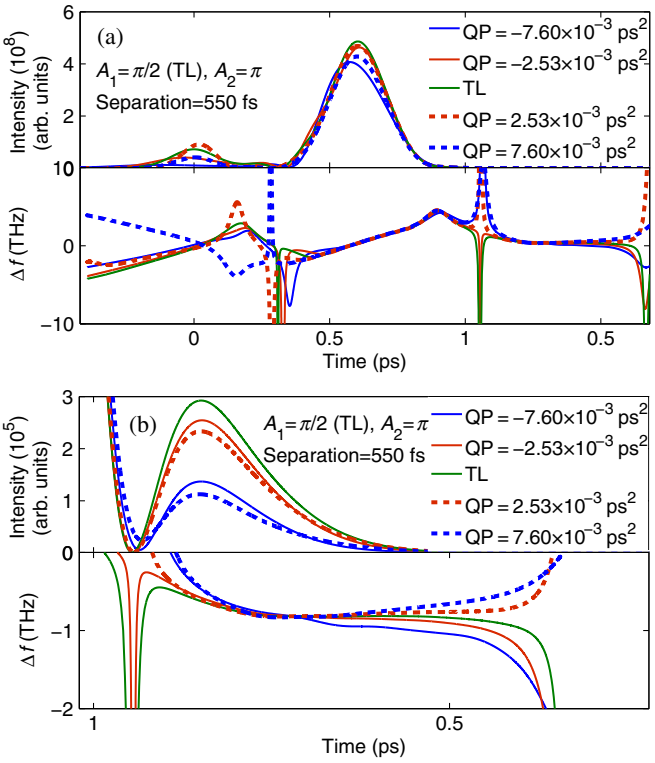

FIG. 5. (a) Simulated output intensity and instantaneous-frequency profiles of excitation and rephrasing (π-area) pulses centered at 1580 nm with varying input QPs of the excitation pulse. The temporal separation between the excitation and rephrasing pulses is 550 fs. (b) Enlarged view of (a) after the rephrasing pulse.

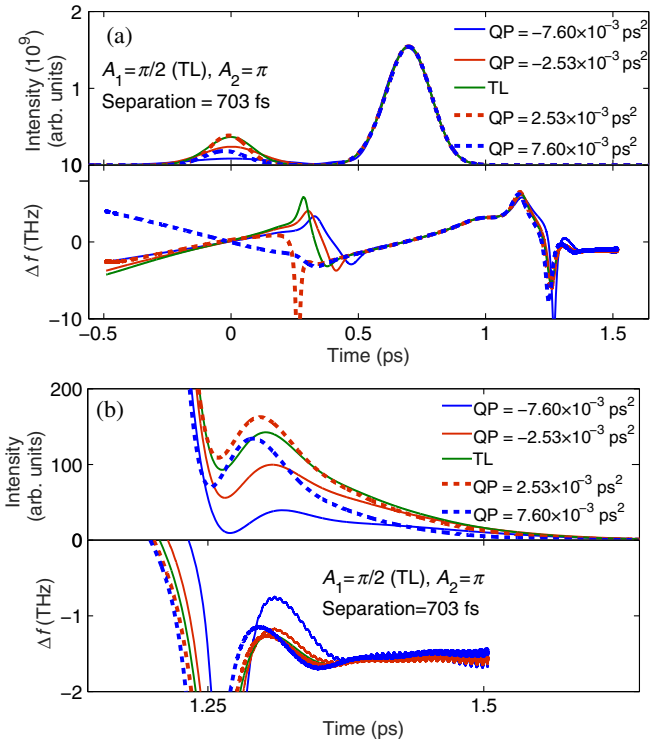

FIG. 6. (a) Simulated output intensity and instantaneous-frequency profiles of excitation and rephrasing (π-area) pulses centered at 1540 nm with varying input QPs of the excitation pulse. The temporal separation between the excitation and rephrasing pulses is 703 fs. (b) Enlarged view of (a) after the rephrasing pulse.

For pulses centered on the short wavelength side of the absorption spectrum, the appearance time and the strength of the echo signal depend strongly on the excitation pulse QPs. In Figs. 6(a) and 6(b), we show the output profiles of pulses centered at 1540 nm and separated temporally by 703 fs. It is clearly seen that the echo signal for the positive QP (negative-chirp) excitation pulse appears earlier and

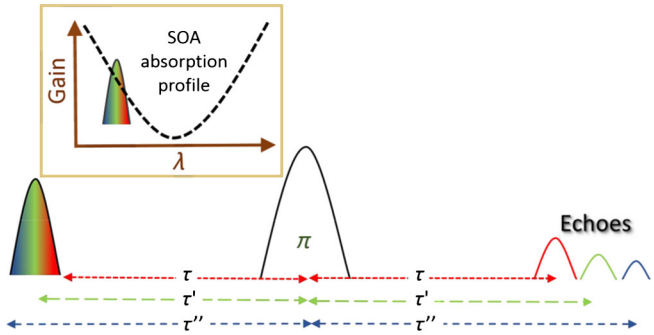

FIG. 7. Schematic explanation of the chirp-induced variation in photon echo for a negatively chirped (QP > 0) first pulse centered at 1540 nm. The inset shows the absorption profile of the QD SOA, and the rainbow representation in the first pulse indicates the negative chirp and the sequence of spectral interaction with the active medium as shown in the inset.

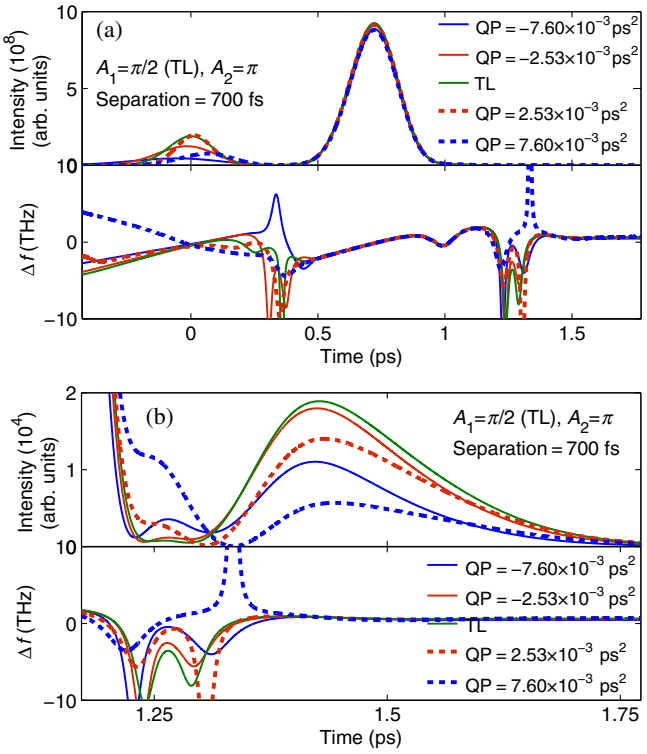

FIG. 8. (a) Simulated output intensity and instantaneous-frequency profiles of excitation and rephrasing (π-area) pulses centered at 1600 nm with varying input QPs of the excitation pulse. The temporal separation between the excitation and rephrasing pulses is 700 fs. (b) Enlarged view of (a) after the rephrasing pulse.

is stronger, while that for the negative QP (positive-chirp) excitation pulse appears later and is weaker, as we describe schematically in Fig. 7. For negatively chirped excitation pulse, the trailing edge of the pulse contains wavelength components that are closer to the SOA absorption minimum (where most of the dipoles lie), and, therefore, the interaction of the pulse with the active medium is strong. The evolution of these trailing-edge excited dipoles are reverted earlier (compared to those of the leading edge) upon interaction with the rephrasing pulse, which results in an earlier-appearing echo with a larger amplitude.

For positively chirped pulse, the leading edge comprises long wavelength components which are closer to the SOA absorption minimum. The decoherence of these longer-wavelength dipoles are reverted at a later time by the π-area rephasing pulse, and this leads to a relatively late-appearing echo signal with a smaller amplitude due to decoherence.

Figures 8(a) and 8(b) present simulated outputs for input pulses separated by 700 fs and centered on the long-wavelength side of the SOA absorption minimum, i.e., at 1600 nm. Because of a sequence of spectral interaction that is the opposite of the one at 1540 nm, a reverse trend is observed in both the appearance time and the strength of the echo signals, as depicted in Fig. 8(b). This concept of inversion of the spectral interaction is the same as we previously reported in regard to Rabi oscillations with chirped pulses [16]. A slight deforming of the shape of the echo signals is observed because of the previously explained interference effects.

IV. CONCLUSIONS

In this work, we present a numerical investigation of a two-pulse photon echo with shaped excitation pulses in an InAs/InP QD SOA having a moderate inhomogeneous broadening. We show that great care needs to be exercised when considering the timing and strength of an echo signal in a distributed systems. We demonstrate that interference leads to a strong dependence of the appearance time and the strength of the echo on the separation between the excitation and the rephrasing pulses, but the two are found to be independent of the excitation pulse area. For an excitation pulse that is centered symmetrically on the absorption spectrum of the QD SOA, the shaping changes only the amplitude of the echo signal, and the medium does not differentiate the interaction sequence introduced by chirping (the QP). By contrast, when the excitation pulse is centered on either the short- or the long-wavelength side of the SOA absorption minimum, the interaction with the medium is asymmetric and any shaping of the optical excitation changes both the appearance time and the amplitude of the echo signal.

The analysis we present establishes that, irrespective of the spectral widths of the QD ensemble gain and of the excitation, the echo can be controlled by appropriately shaped excitation. The observed temporal shifts of the echo signal hold a particular importance where a precise timing of the optical signals matters, which obviously includes the storage and the manipulation of quantum information.

ACKNOWLEDGMENTS

This work is partially supported by the Israel Science Foundation under Grant No. 1504/16. A. K. M. acknowledges the support of the Israel Council for Higher Education. O. K. thanks the Adams Fellowship of the Israel Academy of Sciences and Humanities for the support.

[1] N. A. Kurnit, I. D. Abella, and S. R. Hartmann, Observation of a Photon Echo, Phys. Rev. Lett. **13**, 567 (1964).
[2] D. A. Wiersma and K. Duppen, Picosecond holographic-grating spectroscopy, Science **237**, 1147 (1987).
[3] D. L. McAuslan, P. M. Ledingham, W. R. Naylor, S. E. Beavan, M. P. Hedges, M. J. Sellars, and J. J. Longdell, Photon-echo quantum memories in inhomogeneously broadened two-level atoms, Phys. Rev. A **84**, 022309 (2011).

[4] W. Tittel, M. Afzelius, T. Chanelire, R. L. Cone, S. Krll, S. A. Moiseev, and M. Sellars, Photon-echo quantum memory in solid state systems, Laser Photonics Rev. **4**, 244 (2010).

[5] Jérôme Ruggiero, Jean-Louis Le Gouët, Christoph Simon, and Thierry Chanelière, Why the two-pulse photon echo is not a good quantum memory protocol, Phys. Rev. A **79**, 053851 (2009).

[6] M. Lindberg, R. Binder, and S. W. Koch, Theory of the semiconductor photon echo, Phys. Rev. A **45**, 1865 (1992).

[7] H. Tahara, Y. Ogawa, F. Minami, K. Akahane, and M. Sasaki, Generation of undamped exciton-biexciton beats in InAs quantum dots using six-wave mixing, Phys. Rev. B **89**, 195306 (2014).

[8] P. Borri, W. Langbein, S. Schneider, U. Woggon, R. L. Sellin, D. Ouyang, and D. Bimberg, Ultralong Dephasing Time in InGaAs Quantum Dots, Phys. Rev. Lett. **87**, 157401 (2001).

[9] G. Moody, R. Singh, H. Li, I. A. Akimov, M. Bayer, D. Reuter, A. D. Wieck, and S. T. Cundiff, Fifth-order nonlinear optical response of excitonic states in an InAs quantum dot ensemble measured with two-dimensional spectroscopy, Phys. Rev. B **87**, 045313 (2013).

[10] M. J. Lang, X. J. Jordanides, X. Song, and G. R. Fleming, Aqueous solvation dynamics studied by photon echo spectroscopy, J. Chem. Phys. **110**, 5884 (1999).

[11] P. Borri, W. Langbein, J. M. Hvam, F. Heinrichsdorff, M.-H. Mao, and D. Bimberg, Time-resolved four-wave mixing in InAs/InGaAs quantum-dot amplifiers under electrical injection, Appl. Phys. Lett. **76**, 1380 (2000).

[12] S. V. Poltavtsev, M. Salewski, Yu. V. Kapitonov, I. A. Yugova, I. A. Akimov, C. Schneider, M. Kamp, S. Höfling, D. R. Yakovlev, A. V. Kavokin, and M. Bayer, Photon echo transients from an inhomogeneous ensemble of semiconductor quantum dots, Phys. Rev. B **93**, 121304 (2016).

[13] Saddam Banyoudeh and Johann Peter Reithmaier, High-density 1.54 μm InAs/InGaAlAs/InP(100) based quantum dots with reduced size inhomogeneity, J. Cryst. Growth **425**, 299 (2015).

[14] A. Capua, O. Karni, and G. Eisenstein, A finite-difference time-domain model for quantum-dot lasers and amplifiers in the Maxwell-Schrödinger framework, IEEE J. Sel. Top. Quantum Electron. **19**, 1 (2013).

[15] O. Karni, A. K. Mishra, G. Eisenstein, and J. P. Reithmaier, Nonlinear pulse propagation in InAs/InP quantum dot optical amplifiers: Rabi oscillations in the presence of nonresonant nonlinearities, Phys. Rev. B **91**, 115304 (2015).

[16] Akhilesh Kumar Mishra, Ouri Karni, and Gadi Eisenstein, Coherent control in quantum dot gain media using shaped pulses: A numerical study, Opt. Express **23**, 29940 (2015).

[17] O. Karni, A. K. Mishra, G. Eisenstein, V. Ivanov, and J. P. Reithmaier, Coherent control in room-temperature quantum dot semiconductor optical amplifiers using shaped pulses, Optica **3**, 570 (2016).

[18] D. Hadass, A. Bilenca, R. Alizon, H. Dery, V. Mikhelashvili, G. Eisenstein, R. Schwertberger, A. Somers, J. P. Reithmaier, A. Forchel, M. Calligaro, S. Bansropun, and M. Krakowski, Gain and noise saturation of wide-band InAs-InP quantum dash optical amplifiers: Model and experiments, IEEE J. Sel. Top. Quantum Electron. **11**, 1015 (2005).